アナターゼ型 $ScTiNbO_6$ ナノ粒子の水熱合成

Hydrothermal Synthesis of Anatase-type $ScTiNbO_6$ Nanoparticles

平野正典†, 伊藤貴晴†
Masanori Hirano,† Takaharu Ito†

Abstract A single phase of anatase with composition of $ScTiNbO_6$ was directly synthesized as nano-sized particles from precursor solution mixtures of $Sc(NO_3)_3$, $TiOSO_4$, and $NbCl_5$ under weakly basic hydrothermal condition at 180°C for 5 h in the presence of urea. The lattice parameters of anatase were increased by the replacement of titanium with scandium and niobium, and those values of a_0 and c_0 of new anatase $ScTiNbO_6$ were 0.3902 and 1.0026 nm, respectively. The crystallite size and specific surface area of as-prepared new anatase $ScTiNbO_6$ were 18 nm and 110 m^2g^{-1}, respectively. The optical band gap of anatase-type $ScTiNbO_6$ was 3.59 eV, which was large in comparison with the value 3.22 eV of anatase with pure TiO_2 composition synthesized under the same hydrothermal condition. The single phase of anatase-type $ScTiNbO_6$ existed stably up to 750 °C without an appearance of precipitation of any other phase and phase transition. The low photocatalytic activity of anatase-type $ScTiNbO_6$ was improved in some degree by heat treatment at 750 °C.

1. Introduction

Among the various semiconductor oxides, titania (TiO_2) is an important material for use in a wide range of applications, including photocatalysis and solar energy conversion [1-5]. Various factors, including composition, phase, shape, size, crystallinity, etc. affect the properties of nanocrystalline TiO_2. The crystalline phase, which has been known to show three distinct polymorphs: rutile, anatase, and brookite, affects the majority of the applications of titania. The anatase and rutile are the most intensively investigated phases. The metastable anatase phase usually shows much higher photocatalytic activity than that of the stable rutile one. The properties of titania can be modified via the formation of solid solutions with many dopant materials. The metastable anatase phase generally can form solid solutions with wider composition range than the rutile one. The formation of homogeneous anatase-type solid solutions with dopant by heat treatment above 600 °C via solid-state reaction and sol-gel method is not so easy in general, because pure anatase phase is metastable and easily changes to stable rutile one by heat treatment above 635 °C from the result of the kinetic study [6, 7]. The investigation on the synthesis routes of titania is one of the approaches to achieve a goal. Homogeneous nanocrystalline solid solutions have been prepared via aqueous solution route including hydrothermal treatment [8]. We have investigated on the synthesis and properties of anatase-type TiO_2/SiO_2 composite nanoparticles [9] and SiO_2 gel coated with anatase-type TiO_2 [10] from aqueous $TiOSO_4$ solutions using hydrothermal methods. Anatase-type titania solid solutions doped with iron [11], zirconium[12], niobium [13], and scandium [14] have been directly synthesized from aqueous precursor solutions under hydrothermal conditions. Anatase-type titania solid solutions $Al_XTi_{1-2X}Nb_XO_2$ (X = 0 ~ 0.2) [15] and $Sc_XTi_{1-2X}Nb_XO_2$ (X = 0 ~ 0.2) [16] have also been directly synthesized via aqueous solution route under hydrothermal conditions. Most minerals and compounds having anatase-type structure are TiO_2 or TiO_2 based solid solutions, and that a major part of component consisting of anatase structure is titanium element in general. In our previous studies on the formation of anatase-type $Al_XTi_{1-2X}Nb_XO_2$ and $Sc_XTi_{1-2X}Nb_XO_2$ solid solutions, the major cation part consisting anatase-type solid solutions was titanium element. There has been little information on the presence and synthesis of anatase-type crystal in which Ti component is minor in the composition.

In the present study, we report on a synthesis of anatase-type solid solution in which titanium component is minor in the composition, i.e. a single phase of anatase with composition approximated by $Sc_{0.33}Ti_{0.33}Nb_{0.33}O_2$ (=$ScTiNbO_6$).

2. Experimental

A mixture of an aqueous solution of reagent-grade $Sc(NO_3)_3$, $TiOSO_4$, and ethanol solution of $NbCl_5$ was prepared in a Teflon container. The solution mixture added with aqueous solution of urea was controlled to have a weakly basic condition after hydrothermal treatment by the hydrolysis of urea. The suitable amount of the urea solution was decided as the same amount of H^+ ion concentration produced by hydrolysis of starting metal salts ($Sc(NO_3)_3$, $TiOSO_4$, $NbCl_5$). This solution mixture with total cation concentrations (Sc +

† 愛知工業大学　工学部　応用化学科　(豊田市)

Ti + Nb) of 0.5 mol/dm^3 added with suitable amount of the urea solution in the Teflon container was then placed in a stainless-steel vessel. After the vessel was tightly sealed, it was heated at 180°C for 5 h under rotation at 1.5 rpm. After hydrothermal treatment, the precipitates were washed with distilled water until the pH value of the rinsed water became 7.0, separated from the solution by centrifugation, and dried in an oven at 60 °C. The powders thus prepared were heated in an alumina crucible at heating rate 200 °C/h, held at 700 – 1100 °C for 1 h in air, and then cooled to room temperature in a furnace.

The phases of the as-prepared and heated powders were examined by X-ray diffractometry (XRD; model RINT-2000, Rigaku, Tokyo, Japan) using CuKα radiation. The morphology of the as-prepared samples was observed by transmission electron microscopy (TEM; model JEM-2010, JEOL, Tokyo, Japan). The crystallite size of anatase was estimated from the line broadening of 101 diffraction peak, according to the Scherrer equation, $D_{XRD} = K\lambda/\beta\cos\theta$, where θ is the Bragg angle of diffraction lines; K is a shape factor ($K = 0.9$ in this work); λ is the wavelength of incident X-rays, and β is the corrected half-width given by $\beta^2 = \beta_m^2 - \beta_s^2$, where β_m is the measured half-width and β_s is the half-width of a standard sample. The lattice parameters were measured using silicon as the internal standard. The chemical composition of the resultant powders was analyzed using an inductivity-coupled plasma emission spectrometer (ICP, model; ICP575II, Nippon Jarrell-Ash, Japan). The specific surface area of the prepared samples was calculated from the adsorption isotherm of nitrogen at 77 K based on the Brunauer-Emmett-Teller method (BET, model; NOVA 1200, Yuasa Ionics, Osaka, Japan). The diffuse reflectance spectra measurements for powder samples have been made. The optical absorption of these prepared powders was measured using an ultraviolet-visible spectrophotometer (V-560, Nihon Bunko, Tokyo, Japan).

The photocatalytic activity and adsorptivity of these prepared powders were separately estimated from the change in the concentration of methylene blue (guaranteed reagent grade, $C_{16}H_{18}N_3S$, MB) both under ultraviolet ray (UV) irradiation from black light (20 W), and in the dark, respectively. To 250 cm^3 of aqueous MB solution (5.0×10^{-5} mol/dm^3), 0.05 g of sample powders were dispersed via ultrasonic stirring for 5 min and maintained in the dark for 24 h with stirring. After the dispersed sample powders in the solution adsorbed MB to the full by holding in the dark for 24 h under stirring, the sample in the solution was maintained for 0-5 h under irradiation of ultraviolet ray with an intensity of 1 mW/cm^2 under stirring. Thus, the UV-light irradiation time dependence of MB concentration decomposed by the sample powders was estimated by the measurement of the concentration of MB remained in the solution based on the absorbance change using the spectrophotometer.

3. Results and Discussion

Fig. 1 shows XRD patterns of solid precipitates as-prepared from precursor solution mixture of $Sc(NO_3)_3$, $TiOSO_4$, and $NbCl_5$ under hydrothermal condition at 180 °C for 5 h in the presence of urea. A sample with pure TiO_2 composition as-prepared from precursor solution of $TiOSO_4$ under the same hydrothermal condition is also indicated in the figure to make a comparison. The solid precipitates obtained were detected as single-phase anatase, and no trace of diffraction peaks because of another phase were detected. A shift of the diffraction peaks of the anatase-type TiO_2 to a lower diffraction angle is clearly observed in the sample (Sc, Ti, Nb)O_2 containing niobium and scandium component.

The chemical composition of the single-phase anatase-type sample (Sc, Ti, Nb)O_2 as-prepared from the precursor solution mixture, which was determined by the elemental analysis using an ICP emission spectrometer, is shown in Table 1. The content of titanium in the analytical compositions of the as-prepared samples was slightly more than that in the starting compositions of the samples. We must also reconsider the reliability of the chemical quantitative analysis of water of crystallization (n value) associated in the starting material $TiOSO_4 \cdot nH_2O$, although consideration should also be given to the reliability of the ICP analysis. The synthesized solid precipitate with anatase-type crystalline structure was clarified to have an approximately $Sc_{0.33}Ti_{0.33}Nb_{0.33}O_2$ (=$ScTiNbO_6$) composition. Although we have reported on the formation of anatase-type $Sc_XTi_{1-2X}Nb_XO_2$ solid solutions with X = 0 ~ 0.2 [16], the result in this study shows that the metastable anatase-type TiO_2 can form solid solutions with very wide compositional range (i.e., X = 0.33) in the ternary system Sc_2O_3-TiO_2-Nb_2O_5.

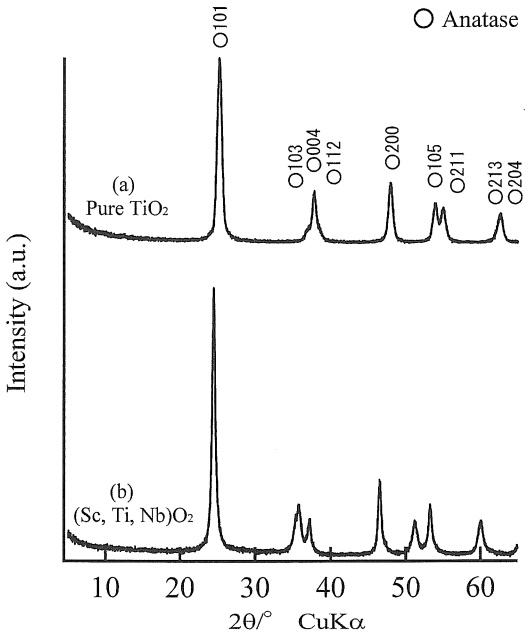

Fig. 1. X-ray diffraction patterns of precipitates obtained from (a) precursor solution of $TiOSO_4$ and (b) solution mixture of $Sc(NO_3)_3$, $TiOSO_4$, and $NbCl_5$ under hydrothermal condition at 180 °C for 5 h.

Starting composition (molar fraction)			Analytical value (molar fraction)		
Sc	Ti	Nb	Sc	Ti	Nb
0.350	0.300	0.350	0.320	0.358	0.322

Table 1. Starting Composition and Analytical Values of Chemical Composition of As-Prepared Anatase-Type Titania Sample in the system Sc_2O_3-TiO_2-Nb_2O_5

Sample	Crystallite size (nm)	BET surface area (m^2g^{-1})	Band gap (eV)	Lattice parameter (nm)	
				a_0	c_0
Pure TiO_2	12.8	123	3.22	0.3789	0.9510
$ScTiNbO_6$	17.6	110	3.59	0.3902	1.0026

Table 2. Crystallite Size, BET Surface Area, Band Gap, and Lattice Parameters of As-Prepared Anatase-Type Titania with Compositions TiO_2 and $ScTiNbO_6$

In Table 2, the lattice parameters a_0 and c_0 of the anatase with $ScTiNbO_6$ composition are summarized in comparison with pure TiO_2 sample obtained under the same hydrothermal condition. The lattice parameters a_0 and c_0 of the anatase fairly increased via containing equal atomic fraction of niobium and scandium to titanium. The corresponding lattice parameter change and the shift of the diffraction lines in the XRD patterns indicated that the anatase-type solid solutions were formed by substituting for titanium sites by niobium and scandium with slightly larger ionic radii than that of titanium, which is supported from the data continually changing in lattice parameters and consideration on the anatase-type $Sc_XTi_{1-2X}Nb_XO_2$ solid solutions with $X = 0 \sim 0.2$ [16]. An anatase in which titanium component was minor in the composition was synthesized under this experimental condition.

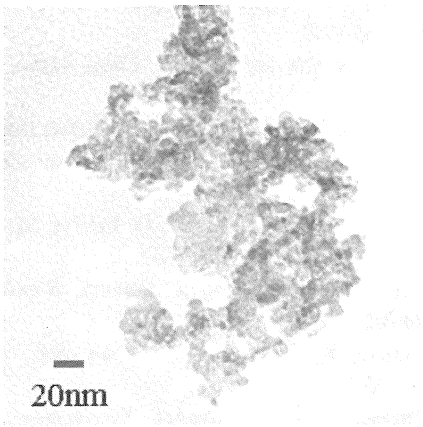

Fig. 2. Transmission electron microscopy image of as-prepared anatase-type $ScTiNbO_6$.

A TEM image of the as-prepared anatase-type $ScTiNbO_6$ is shown in Fig. 2. The crystallite size of anatase-type $ScTiNbO_6$ estimated from the XRD line broadening and its specific surface area is also shown in Table 2. The crystallite size of anatase estimated from the XRD line broadening corresponded relatively well to the particle size of the samples estimated from the TEM observation. The anatase-type $ScTiNbO_6$ was synthesized as nanocrystalline particles from the precursor solution mixture. The diffuse reflectance spectra of the as-prepared anatase-type $ScTiNbO_6$ and pure TiO_2 are shown in Fig. 3. The shift of the onset of absorption to shorter wavelengths was observed in the sample anatase-type $ScTiNbO_6$ in comparison with that of pure TiO_2. A band-gap value for the anatase-type $ScTiNbO_6$ is shown in Table 2, which was determined from the energy intercept by extrapolating the straight regions of the plot of $(\alpha h\nu)^2$ versus the photon energy $h\nu$ for a direct allowed transition (E_d), as compared with pure TiO_2 sample hydrothermally prepared under the same condition. The optical band-gap value of anatase $ScTiNbO_6$ is found to be fairly large by comparing with that of pure TiO_2.

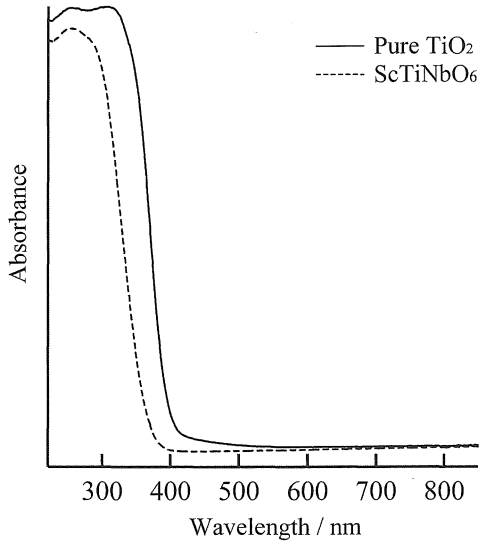

Fig. 3. Diffuse reflectance spectrum of as-prepared anatase-type TiO_2 and $ScTiNbO_6$.

Phase stability of anatase with composition $ScTiNbO_6$ synthesized as nanoparticles was investigated. XRD patterns of the $ScTiNbO_6$ precipitate before and after heating at 750 °C for 1 h are shown in Fig. 4. The solid precipitate after heat treatment at 750 °C for 1 h was detected as single-phase anatase, and no trace of diffraction peaks because of another phase were detected. No change was also detected in crystalline phase in the sample through the heat treatment although a change in sharpness in diffraction peaks due to crystallite growth of anatase was observed. This result indicates that the $ScTiNbO_6$ can exist stably as a single phase of anatase up to 750 °C. By heat treatment in air above this temperature new anatase $ScTiNbO_6$ was transformed into single and stable phase [17].

The photocatalytic activity for the as-prepared anatase-type $ScTiNbO_6$ and reference anatase-type pure TiO_2 (ST-01) was estimated as changes in the concentration of MB with time in the dark and under UV-light irradiation. The photocatalytic activity of as-prepared anatase-type samples is shown in Fig. 5 as plots of $-\ln(C/C_0)$ versus UV-light irradiation time. The photocatalytic activity of anatase-type $ScTiNbO_6$ is improved in some degree by

heat treatment at 750 °C but it is lower than those of anatase-type pure TiO_2 and ST-01 as reference samples.

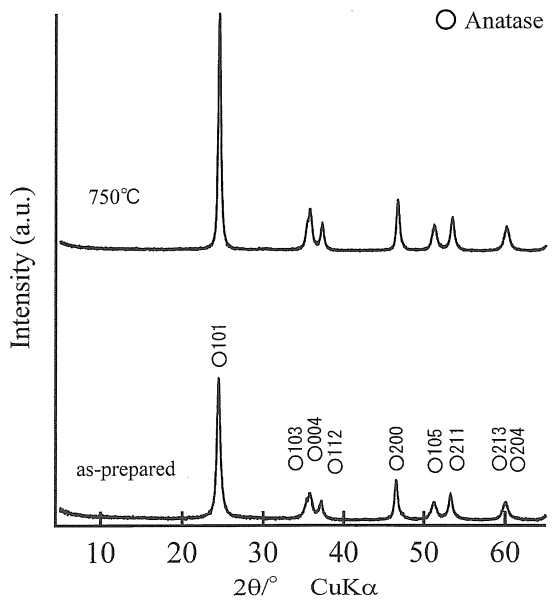

Fig. 4. X-ray diffraction patterns of the $ScTiNbO_6$ precipitate before and after heating at 750 °C for 1 h.

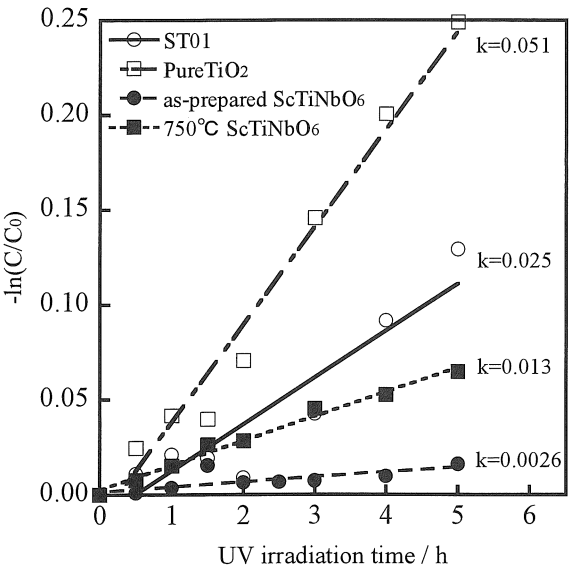

Fig. 5. Photocatalytic degradation of methylene blue as a function of ultraviolet irradiation time for as-prepared $ScTiNbO_6$, heat treated $ScTiNbO_6$, and reference samples (as-prepared anatase-type TiO_2 and ST-01).

4. Summary

A single phase of anatase with composition approximated by $Sc_{0.33}Ti_{0.33}Nb_{0.33}O_2$ (=$ScTiNbO_6$), in which titanium component was minor in the composition, and that containing equal atomic fraction of niobium and scandium to titanium, was directly synthesized as nanocrystalline-particles from precursor solutions of $TiOSO_4$, $NbCl_5$, and $Sc(NO_3)_3$ under weak basic hydrothermal condition at 180 °C for 5 h in the presence of urea. The lattice parameters a_0 and c_0 of anatase $ScTiNbO_6$ were 0.3902 and 1.0026 nm, respectively. The optical band gap of anatase-type $ScTiNbO_6$ was 3.59 eV. The compound $ScTiNbO_6$ can exist stably as a single phase of anatase up to 750 °C. The anatase-type $ScTiNbO_6$ showed low photocatalytic activity.

References

1. A. Fujishima and K. Honda, *Nature (London)*, **238** (1972) 37-38.
2. M. A. Fox and M. T. Dulay, *Chem. Rev.*, **93** (1993) 341-357.
3. U. Bach, D. Lupo, P. Comte, J. E. Moser, F. Weissortel, J. Salbeck, H. Spreitzer, M. Graetzel, *Nature*, **395** (1998) 583-585.
4. B. O'Regan , M. Graetzel, *Nature*, **353** (1991) 737-740
5. P. V. Kamat , N. M. Dimitrijevic, *Solar Energy*, **44** (1990) 83-98.
6. A. W. Czanderna, C. N. R. Rao, and J. M. Honig, *Trans. Faraday. Soc.*, **54** (1958) 1069-1073.
7. S. R. Yoganarasimhan, C. N. R. Rao, *Trans. Faraday. Soc.*, 58 (1962) 1579-1589.
8. M. Hirano, T. Miwa, and M. Inagaki, *J. Am. Ceram. Soc.*, **84** (2001) 1728-1732.
9. M. Hirano, K. Ota, and H. Iwata, *Chem. Mater.*, **16** (2004) 3725-3732.
10. M. Hirano and K. Ota, *J. Mater. Sci.*, **39** (2004) 1841-1844.
11. M. Hirano, T. Joji, M. Inagaki, H. Iwata, *J. Am. Ceram. Soc.*, 87 (2004) 35-41.
12. M. Hirano, C. Nakahara, K. Ota, O. Tanaike, M. Inagaki, *J. Solid State Chem.*, 170 (2003) 39-47.
13. M. Hirano, K.Matsushima, *J. Nanosci. Nanotechnol.*, 6 (2006) 762-770.
14. M. Hirano, K. Date, *J. Am. Ceram. Soc.*, 88 (2005) 2604-2607.
15. M. Hirano, T. Ito, *J. Nanosci. Nanotechnol.*, 6 (2006) 3820-3827.
16. M. Hirano, T. Ito, *Mater. Res. Bull.*, 43 (2008) 2196-2206.
17. M. Hirano, T. Ito, *J. Solid State Chem.*, 182 (2009) 1581-1586.